RSC Advances

ROYAL SOCIETY OF CHEMISTRY

www.rsc.org/advances

Cite this: DOI: 10.1039/c0xx00000x

www.rsc.org/xxxxxx

ARTICLE TYPE

Design and fabrication of surface-enhanced Raman scattering substrate from DNA-gold nanoparticles assembly with 2-3 nm interparticle gap

Li Zhang *[a], Hongwei Ma,[b] Liangbao Yang [c]

Received (in XXX, XXX) Xth XXXXXXXXX 200X, Accepted Xth XXXXXXXXX 200X

DOI: 10.1039/b000000x

An ideal substrate for surface-enhanced Raman scattering (SERS) detection should induce a high signal enhancement and be easy to synthesize. Here, we showed that gold nanoparticles (Au NPs) were self-assembled onto the DNA strands through electrostatic interactions and formed a well-defined DNA-Au hybrid structure with an interparticle gap of ca. 2-3 nm between two adjacent Au NPs, which could be used as active SERS substrates. Four different types of molecules, i.e. Rhodamine 6G, 4-aminothiophenol, pyridine and 2, 4, 6-trinitrotoluene were studied on these substrates. All the detection limits for each analyte on the DNA-Au hybrid substrate were at least one order of magnitude higher than that on the Au NPs solely without the self-assembly on DNA. This phenomenon of assembly-induced signal enhancement had been experimentally and theoretically demonstrated in this study.

1. Introduction

The control of interparticle interactions and structures in nanoparticle assemblies using organic molecules or biomolecules as the mediators has attracted increasing interests towards the design of functional nanostructures.[1–4] In particular, the design and fabrication of these functional nanostructures have been widely explored for the signal amplification in the field of surface-enhanced Raman scattering (SERS).[5] For conventional SERS substrates, the interstitial size is difficult to control owing to the stochastic distribution of the nanoparticles (NPs). Both experimental and theoretical results indicated that the precise control of the gaps among the nanostructures in the range of sub-10 nm was critical for the preparation of the SERS substrates with high enhancement factors, especially 1–3 nm for optimal coupling of the electromagnetic field.[6-9,] Some efforts[10, 11,] have demonstrated the great potential of SERS as a sensitive tool for the molecular sensing, however, the precise control of the gaps in the sub-10 nm range on a SERS-active substrate for intense SERS enhancement is still a huge challenge base on the state-of-art technology.

The biomolecular structures are attractive as templates to form nanoscale architectures because of their size, geometry and ability to interact with inorganic materials.[12] DNA molecule is a kind of attractive biological templates to construct nanostructures with a specific shape and unique properties. DNA is a rigid biopolymer that can withstand a range of pH, temperature. Particularly, DNA possesses a linear structure, large aspect ratio (length/diameter), well-defined sequences, and a variety of superhelix structures. The negatively-charged phosphate groups of DNA have a strong affinity to bind the metal cations and positively-charged NPs.[13] In addition to the linear structure, large-scale DNA networks can also be fabricated by controlling DNA concentration.[14] A large-scale λ-DNA network on a mica surface was successfully fabricated through a self-assembly method.[15] Recnetly, we have reported a sunlight-induced formation of silver-gold bimetallic nanostructures on DNA template for highly active SERS substrates and application in TNT/tumor marker detection,[16] and we have also studied the DNA-Ag hybrid structure for ultratrace mercury analysis.[17]

To date, the challenges are how to synthesize the SERS substrates with a gap of ca. 2-3 nm in solution and how to control the uniform distribution of the hot spots and the uniformity of SERS nanostructures.[18-22] Here, a very simple and practical strategy was experimentally and theoretically demonstrated for the high-yield synthesis of a new kind of nanostructures with a well-defined 2-3 nm interparticle gap between two adjacent Au NPs by the self-assembly of Au NPs on DNA (Fig. 1). The anchored DNA strands in these particles facilitated the formation of the nanogaps. This kind of nanogaps among the Au NPs surface resulted in the amplification of the SERS signal intensity.

2. Experimental section

2.1 Materials and chemicals

300 ng/μl λ-DNA was purchased from Fermentas Life Sciences Ltd. Company (Shenzhen, China) and was extensively dialyzed in pure aqueous solution. All chemicals used in this study were of analytical grade. $HAuCl_4 \cdot 3H_2O$ was obtained from Shanghai Chemical Co. Ltd. China. All the solutions were prepared in double distilled water.

2.2 Characterizations

Ultraviolet-visible (UV-Vis) absorption spectra were collected on a Solidspec-3700 spectrophotometer. The transmission electron microscopy (TEM) images were obtained with a JEOL JEM-2010 instrument operated at 100 kV. SERS measurements were carried out on a Labram I confocal microprobe Raman system (JY,

France). The excitation wavelength is 532 nm. All of the spectra reported were the results of a single 2 s accumulation. AFM measurements were performed with a digital Nanoscope IIIa multimode system (DI, Santa Barbara, CA). The image was acquired in the tapping mode. The AFM measurements were performed in air at room temperature with a Si cantilever. The force constant of the cantilever was 0.1–0.6 N/m with the scan rate at 1–2 Hz.

2.3 Preparation of DNA-Au hybrids

Positively charged Au NPs with diameters of about 6 nm were prepared by the phase transfer approach following the procedure of Gittins and colleagues.[23] The fabrication of the network nanostructure was carried out as our former study.[16] An aqueous solution of positively charged Au NPs was added to a solution of λ-DNA (20 mL, 300 ng/μl, the diluted DNA solution is about 50 ng/μl) and the solution was mixed thoroughly and kept for 3 h at room temperature. The **DNA** solution changed into wine red, indicating the formation of DNA-Au hybrids. The precipitate, i.e. the synthesized DNA-Au hybrid, was resuspended and centrifuged with distilled water three times and then ultrasonically dispersed into distilled water.

2.4 SERS measurements on the DNA-Au network films

1 ml of the as-prepared DNA-Au NPs hybrid solution was centrifuged at 8000 rpm for 10 min. The supernatant was discarded, and the pellet was re-dispersed as 10 ml. 10 μl of the as-prepared DNA-Au hybrid was dropped onto the surface of a silicon wafer and dried in air as the SERS substrate. The dried DNA-Au network film has a diameter of ca. 2 mm. 1 ml of the positively charged Au NPs solution was centrifuged at 16000 rpm for 30 min and the pellet was re-dispersed as 10 ml. The following steps are similar to the above. Using Rhodamine 6G (R6G) stock solutions of 10^{-3} M, we prepared solution with concentrations down to 10^{-6} M via successive dilution by factor of 10. After immersing the SERS substrates into the corresponding solution for some time in order to ensure that the adsorption equilibrium was reached, the substrates were then taken out, rinsed with deionized water. The samples were dried in air. In order to avoid the catalytic and photochemical decomposition caused by laser exposure, the laser power at the sample position was 0.5 mW, the laser beam was focused on the sample in a size of about 2 μm and the typical accumulation time used for the study was 2 s. For every sample, we took three SERS spectra in different position of the substrate and then averaged them. Similarly, a series of concentrations of 4-aminothiophenol (4-ATP) pyridine (Py) and 2, 4, 6-trinitrotoluene (TNT) were prepared. The condition of their SERS measurements is similar to the protocol of R6G SERS detection.

3. Results and discussion

3.1 DNA-based fabricating of DNA-Au hybrids

This study provides a one-step strategy for preparing DNA-Au hybrids as SERS active substrates by simple mixing of DNA and Au colloids. Our strategy on the self-assembly of Au NPs on DNA template can be summarized as follows: Firstly, the positively-charged Au NPs was synthesized through a phase transfer method,[23] which had a diameter of c.a. 6 nm as observed by TEM (Fig. 1A); Secondly, the as-synthsized Au colloids were mixed with the λ-DNA aqueous solution to obtain the highest density of the self-assembly of DNA-Au hybrids (Fig. 1B); Thirdly, the Au NPs were self-assembled onto the DNA strands by electrostatic interactions between the negatively-charged phosphate backbones of DNA and positively-charged Au NPs; Finally, DNA network provides a good template for the formation of compact and uniform nanostructures by the electrostatic assembly of Au NPs on DNA strands. In a typical experiment, because the negatively-charged phosphate groups as the backbone of DNA molecule have a linear shape of periodic arrangement and have a strong affinity to the positively-charged Au NPs, the DNA strands can be used as a template with the highly-accurate position-controlling capability which finally resulted in the self-assembly of DNA-Au hybrids with 2-3 nm interior gap (Fig. 1B). Importantly, the HRTEM images (inset in Fig. 1B) verified that Au touched to DNA surface in some parts to form DNA-Au chain. The final hybrids were successfully fabricated in a high yield of ca. 95% and all particles had a uniform nanogap as shown in the TEM images in Fig. 1B. The average gap size, measured from the TEM images, was determined to be 2-3 nm (Fig. 1D). The synthesized DNA-Au nanostructures were highly stable in solution over three months in ambient conditions. All these characteristics were very important for SERS detection. As shown in Fig. 1C, the DNA absorption peak appeared at 256 nm (curve 1). Compared with curve 1 in Fig. 1C, the intensity of the DNA-Au hybrid absorption peak in curve 3 red-shifted to 277 nm. Because of the intimate nature of the DNA-Au complex, this effect could be attributed to the changes in the duplex structure,[16] and therefore the new peak at 277 nm is attributed to the interaction between the groups of DNA and the surface atoms of positively charged Au NPs.[23] In curve 2, the peak at 509 nm can be attributed to the surface plasmon resonance of small Au NPs. From curve 3, the plasmon resonance peak red-shifted to 526 nm with a broader shape owing to the complete DNA-Au hybrid formation, but the extinction intensity had increased compared with the Au NPs. The color of the particle solution deepened as shown in the inset of Fig. 1C.

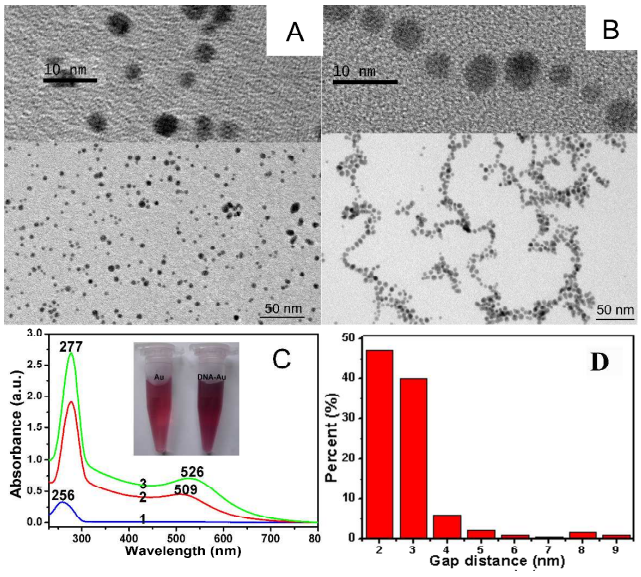

Fig. 1 DNA-mediated fabricating and characterization of DNA-Au hybrids. A and B: TEM of the positively charged Au NPs and using DNA-modified Au NPs forming DNA-Au hybrids, respectively. The inset

is high-resolution TEM image. C: UV-vis spectra for the solution of: DNA (curve 1), positively charged Au NPs (curve 2) and DNA-Au hybrids (curve 3). Inset: gradual change in the color of the solution. D: Percent of the gap distance of Au NPs on DNA template. A section analysis reveals the gap of the particles is about 2-3 nm.

Fig. 2 showed typical TEM images of self-assembled DNA-Au nanostructures obtained by absorbing Au NPs onto the DNA networks with different volume ratios from 4:1 to 1:1, respectively. There were some single Au NPs in the solutions as shown in Fig.2A and 2B. It was clearly visible from the TEM images in Fig.2C and 2D that almost every chain was decorated with a high density of Au NPs. The measured distance of the particles attached to the DNA chains was in the range of 2 to 3 nm, which falled into the size range of the Au NPs we used for the assembly of SERS substrate. The result showed that the optimal volume ratio was about from 2:1 to 1:1. It was necessary to point out that, if the colloid concentration was too low, it was difficult to absorb sufficient NPs on the DNA chains. However, if the colloid concentration was too high, large dissociative NPs will form rapidly when the NPs are injected into the DNA solution.[24] In this study, 300 ng μl^{-1} λ-DNA containing 48,502 base pairs was extensively dialyzed in pure aqueous solution. In each sample, the final concentration of λ-DNA is 50 ng μl^{-1}. Based on this calculation, 26 DNA bases per one nanopaeticles is the optimum ratio. To further identify the particles assembled on the DNA chains, Au NPs with different diameters (such as 15nm and 25nm) were also chosen for the assembly. The results showed that, only some DNA chains were decorated by many particles, and the nanogap among the Au NPs was not uniform (details were shown in supporting information, Figure S1), which further verified that the size of the NPs was the key factor for the successful assembly of our strategy. It was obvious that the interactions between DNA and NPs were predominant. By using this specific characteristic of DNA and Au NPs, we have fabricated Au NPs decorated DNA nanowires or nanochains. Without question, many factors will affect the electrostatic assembly of Au NPs on DNA strands. In this work, the main purpose is to provide a simple and efficient strategy for the preparation of SERS substrates. The strategy we have developed in this work does not require any chemical modifications (e,g, introducing special chemical groups) to the DNA chains for the assembly. Therefore, it minimizes any possible changes to the native properties of DNA, which is very important for SERS.

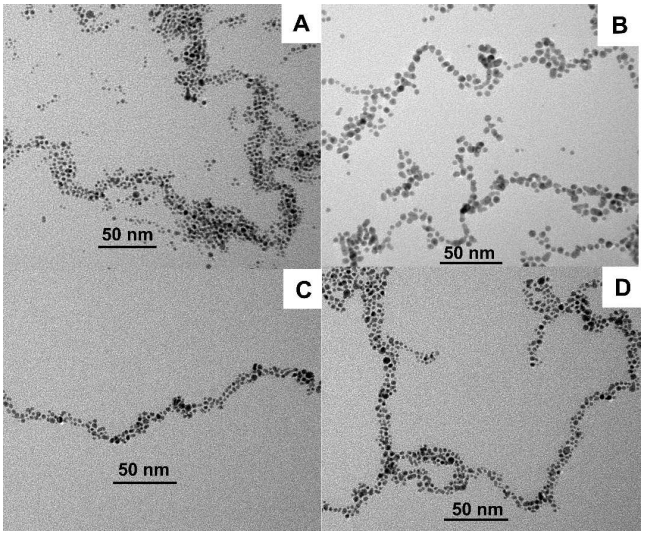

Fig. 2 Typical TEM images of the mixtures of Au NPs and DNA solution with different volume ratios: (A) 4:1, (B) 3:1, (C) 2:1 and (D) 1:1(Au NPs: DNA). [DNA]=50 ng/μl.

Fig.3A showed the UV-Vis spectra recorded from a mixture of 50 ng/μL DNA and different concentrations of Au NPs. Prior to mixing, it can be seen that there was a same peak at about 509 nm with increasing concentration from line 1 to line 3, whereas a absorption peak was observed at around 526 nm after mixing, the absorption peak at 509 nm red-shifted toward longer wavelength in the presence of DNA template and there was no other peak arising. UV-vis spectra of DNA-templated NPs self-assembled with different DNA concentrations were also shown in Fig.3B. The absorption peaks still red-shifted toward longer wavelength from 509 nm to 526 nm in the presence of DNA template with increasing concentrations and there was no other peak arising, which was not similar to the literature.[25] The established theoretical descriptions of Mie scattering from similar small aggregate clusters suggested that the plasmon resonance absorption of the aggregates would have an additional long wavelength component in the optical absorption spectrum relative to the absorption from isolated NPs dispersed in solutions.[26] The first peak, located near the resonance peak of monodispersed particles, was attributed to the quadrupole plasmon excitation in coupled NPs, the other peak at a longer wavelength was attributed to the dipole plasmon resonance of the NPs aggregate.[27]

However, in our study, the new absorbance peaks at 526 nm did not further shift to much longer wavelength as increasing gold concentration. We attributed this phenomenon to the NPs self-assemblies in a linear shape rather than their aggregations. On the other hand, there was no longitudinal absorbance mode. That is to say, the assembled Au NPs were discontiguous, which was in agreement with the TEM observations.

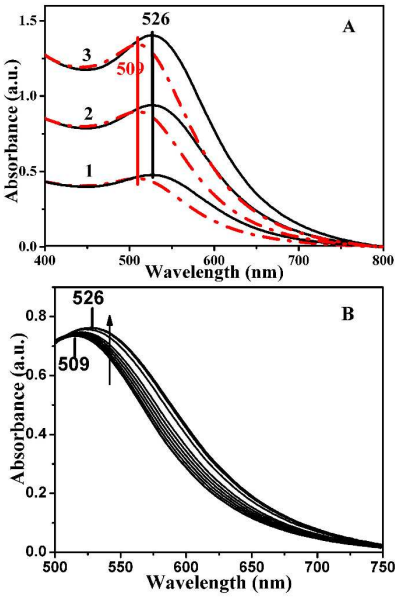

Fig. 3 (A) UV–vis spectra of Au NPs (dashed line) and DNA-Au (real line) with different volume ratios of Au NPs and DNA, [DNA]=50 ng/μL, volume ratios of line 1, 2 and 3 corresponding to 4:1, 3:1, 2:1, respectively. (B) UV–vis spectra recorded for an aqueous mixture of DNA-Au complex with increasing DNA concentration from 50 ng/μL to 100 ng/μL.

Optical waveguide (OWG) spectroscopy is a new and powerful technique for surface monitoring. The technique takes advantage of the evanescent field, which penetrates less than a wavelength out of the waveguide surface, to selectively respond to the adsorption of immobilized chemical or biological molecules over a given spectral bandwidth. Here, λ-DNA is stretched, aligned, and immobilized on an optical waveguide glass surface by the molecular combing method.[28] By adding Au colloids on the DNA modified glass surface, we used the OWG spectroscopy to monitor the Au NPs dynamic assembly process through the electrostatic interactions between the negatively charged phosphate backbone and positively charged Au NPs. Through the OWG absorption spectroscopy, the time of adsorption equilibrium was determined, and the Au NPs adsorption process in the solid-liquid interface followed diffusion control theory. Fig.4A showed the single-layer assembly of Au NPs, resulting in the appearance of an absorbance peak centered at ca. 527 nm, which could be attributable to the located surface plasmon resonance (LSPR) peak of the adsorbed Au NPs. Even if we prolonged the reaction time, there was not a redshift of this LSPR or the appearance of new peaks at longer wavelengths which were attributed to the coupling, multilayer assembling, or aggregating of Au NPs on the OWG surface.[29] At the same time, the intensity of the absorbance does not increase, which was in agreement with the result of Fig.3, it means that electrostatic interactions are the key factor during the process.

As reported in previous articles, the height of double-stranded DNA spread on mica was about 0.4-0.7 nm measured by AFM in tapping mode. When the DNA concentration is 50 ng/μL, the DNA strands can form single chain or netlike structure. A section analysis indicated that the strand height was about 2 nm (date not shown). Fig.4B showed typical AFM images of DNA-Au networks with 50 ng/μL DNA. The image clearly confirmed that Au NPs were absorbed onto the DNA strands with high specificity. It was also found that the assembled Au NPs were denser along the DNA strands. The height of DNA-Au networks was in the range of 7.8 nm to 15.5 nm. This results indicated that two DNA strands or more overlapped each other at the concentration of 50 ng/μL,[15] another reasonable explaination may be that two Au NPs were anchored to the same location of DNA strands. It should be noted that the dimensions of the particles were measured according to the height rather than the width, because the AFM tip radius would affect the measurement.

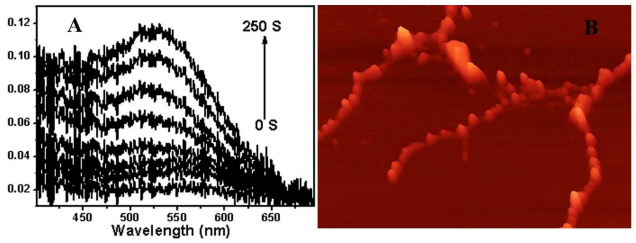

Fig. 4 (A) Assembly process of single-layer Au NPs on DNA-modified OWG surface. (B) Tapping-mode AFM images of self-assembled films of DNA-Au obtained by absorbing Au NPs onto a DNA, [DNA]=50ng/μL.

3.2 Scheme of the fabrication of the gold-decorated DNA template and DDA simulation of optical electric-field distribution

On the basis of the TEM and AFM results above, it was believed that the formation of the DNA-Au hybrid structures mainly resulted from the directing effect provided by the reaction between gold and Au NPs, Au NPs and DNA. The maximum amount of the Au NPs tethered on DNA template were determined by the space charge repulsion of positively charged Au NPs and by electrostatic interactions between the negatively charged phosphate backbone of DNA and the positively charged Au NPs. Our earlier study found that λ-DNA can form cross-chain structure and single chain structure.[16] In this study, the similar phenomenon was observed. According to the experimental results above, a possible formation mechanism of the DNA-Au hybrid structure was proposed as shown schematically in Fig.5, including the cross-chain (A) and the chain (B) modes of DNA-Au complex. In our model, we supposed that the Au NPs were configured to the plane of the phosphate DNA backbone. Our reason is that the phosphodiester backbone is a linear shape of negative charge compensated by the counter Au NPs. The negative charge repulsion is by no means completely screened by the counter charge since the Debye screening length about 1.8 nm, because the solution conditions used here are significantly larger than the distance bewtween two adjacent phosphate groups (max. 0.76 nm).[30] On the other hand, the positively charge repulsion of Au NPs also exists. In our experiments, we found that the distance of Au NPs among the DNA template is about 2-3 nm.

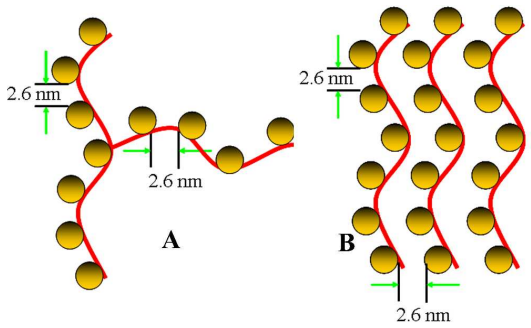

Fig. 5 Proposed self-assembly structures of DNA-Au (A) cross-chain structure, (B) chain structure.

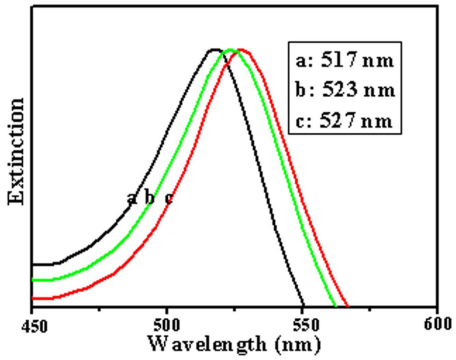

Fig. 6 The calculated extinction efficiencies of Au NPs. Curve a: single particles, curve b: on cross-chain, curve c: on chain DNA. The nanospheres have a diameter of 6 nm.

In order to understand the mechanism and to calculate the field enhancement, a theoretical simulation was carried out by using the DDA method. The extinction spectra of the Au NPs solely, the Au NPs assembled on cross-chain DNA template, and the Au NPs assembled on chain DNA template with a gap of 3 nm were calculated using DDA method in Fig.6. The corresponding SPR peaks were at 517 nm (curve 1), 523 nm (curve 2) and 527 nm (curve 3). We noticed that the SPR peak of 527 nm was just located at the wavelength of the excitation line of 532 nm and was more suitable in the present study. Then we calculated the local electric field distribution of the Au NPs without or with DNA templates. Fig.7A-7C showed the local electric field distribution of the Au NP solely, the Au NP assembled on cross-chain DNA template, and the Au NPs assembled on chain DNA template, respectively. The calculated results revealed that the magnitude of the maximally enhanced electric field is about 6 times for single Au NP, about 7 times for Au NPs with a cross-chain structure, and about 8 times for Au NPs with a chain structure. The highest enhancement of Raman scattering appeared at the surface and the junction with magnitudes of about 1296, 2401 and 4096 fold, respectively. It should be pointed out that a great deal of chain-like gold nanostructures existed, i.e. the assembly of DNA-Au hybrid had a high yield (see Fig.1b and Fig.2). As this structure increased, the number of "hot junctions" increased, and thus a more intense SERS band was produced. As the NPs became very close with the controllable gaps, the LSPR can be excited in the well-controlled nanogap. Hence, it produced a large electromagnetic field enhancement and a tremendous increase of the Raman intensity for molecules located in the gap of the particles, and thus allowed the detection of monolayer adsorbed species on a practically important substrate of general interest. Thus, we considered the gap effect was the dominant factor for the field enhancement.

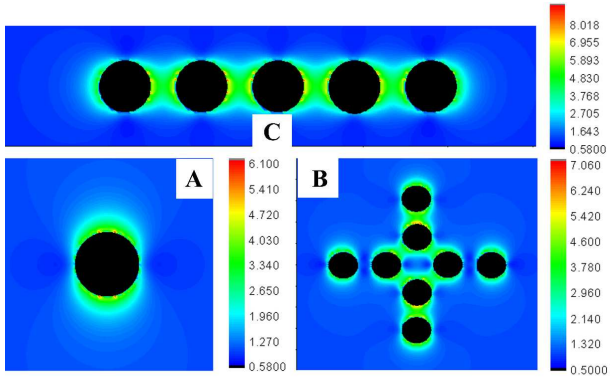

Fig. 7 DDA simulation of the field-enhancement of gold NPs (A) single, (B) on cross-chain DNA, (C) on chain DNA, respectively. The wavelengths are chosen as their own resonant wavelengths (517 nm, 523 nm, and 527 nm, respectively).

3.3 SERS studies of DNA-Au substrate

Several types of typical analytes were selected as models to demonstrate the performance of this substrate in SERS because they are important and have been well-characterized by SERS.

Fig.8A showed the intensity of SERS spectra of R6G with different concentrations from 1.0×10^{-5} to 1.0×10^{-6}M. The spectral features of R6G molecules were existed: the peak at 1189 cm^{-1} is associated with C-C stretching vibrations, and the peaks at 1311, 1359, 1507, 1571 and 1644 cm^{-1} were associated with aromatic C-C stretching vibrations. The Raman bands at about 1644, 1507, 1359, 1189, 770, and 611 cm^{-1} can be attributed to R6G and agreed well with literature data.[31,32] Comparing curve 1 with curve 3, Raman peak strongly decreased in intensity as the concentration of R6G decreased, and was clearly observable at the concentration as low as 1.0×10^{-6} M on the DNA-Au substrate. This indicates that DNA-Au as SERS substrates provide strong Raman signals of R6G. Comparing curve 2 with curve 3, we believe that this specific SERS substrate is more reasonable than the Au substrate with the same size.

Fig. 8B presented the SERS spectra of 4-ATP on the substrates formed by the Au NPs solely and the DNA-Au hybrid, respectively. A strong band can be observed at ca. 1075 cm^{-1}, which was assigned to C(benzene ring)-S stretching vibration, while the relational band located at 1570 cm cm^{-1} was assigned to C–C stretching vibration of benzene rings. The band at 1005 cm^{-1} was originated from C–C bending vibration, and the bands at 1185 cm^{-1} and 1469 cm^{-1} was originated from the C–H bending vibration and a combination of C–C stretching and C–H bending vibration, respectively. Moreover, the bands located at 1139 cm^{-1} and 1429 cm^{-1}, which were ascribed to the charge transfer from the metal to the adsorbed molecules, could also be seen clearly, and it suggested a perpendicular orientation of 4-ATP unit to the metal surface [33]. From curve 1, curve 2 and curve 3 of Fig. 8B, we could see that curve 3 and curve 2 had the better spectral quality with more peaks and higher signal intensities, while curve 1 had relatively weaker signals and some peaks were disappeared. Comparing curve 1 with curve 2, the detection limit of 4-ATP by SERS on DNA-Au substrate is at least one order of magnitude

higher than that on the Au NPs solely at the same conditions.

Fig.8C presented the SERS spectra of Py. The spectra had strong Py bands at ca. 652, 995, 1033, 1216 and 1582 cm^{-1}. These spectra agreed very well with those reported in previous works.[34] These five bands are assigned to totally symmetric vibrational modes, indicating that Py adsorption made the aromatic ring normal to the surface. From curve 1, curve 2 and curve 3 of Fig.8C, it could be noted that the signal of Py was about one order of magnitude higher on DNA-Au substrate than that on Au NPs solely.

To demonstrate that the sensitive detection of the DNA-Au substrates was widely applicable, we further measured the Raman spectra of TNT. The detection and identification of trace TNT was a problem of great practical interest. The peak at 1609 cm^{-1} was due to the C=C aromatic stretching vibration. The strong Raman band at 1359 cm^{-1} was due to the NO_2 symmetric stretching vibration and the weak band at 1532 cm^{-1} was due to the NO_2 asymmetric stretching vibration, and the band at 1210 cm^{-1} (C_6H_2-C vibration). Out of plane vibrations can be seen at 792 and 822 cm^{-1} at a modest intensity. All of these were due to TNT vibration.[35, 36, 37] Fig. 8D demonstrates that DNA-Au substrate can be detected in concentration ranges down to 10^{-5} M of TNT.

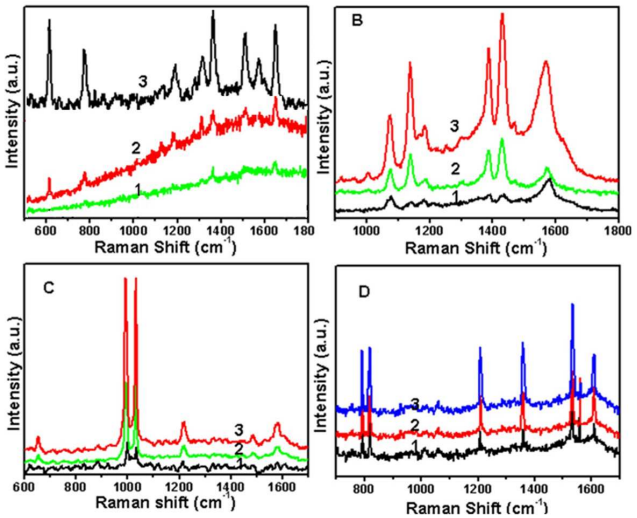

Fig. 8 Typical SERS spectra of different concentration of analyte molecules on different SERS substrate, (A) R6G, curve 1: DNA-Au substrate, 10^{-5} M, curve 2: Au substrate, 10^{-5} M, curve 3: DNA-Au substrate, 10^{-6} M. (B) 4-ATP. Curve 1: Au substrate, 10^{-5} M, curve 2: DNA-Au substrate, 10^{-6} M curve 3: DNA-Au substrate, 10^{-5} M. (C) Py, curve 1: Au substrate, 10^{-5} M, curve 2: DNA-Au substrate, 10^{-7} M, curve 3: DNA-Au substrate, 10^{-6} M, (D) TNT, curve 1: Au substrate, 10^{-4} M,curve 2: DNA-Au substrate, 10^{-5} M, curve 3: DNA-Au substrate, 10^{-4} M.

4. Conclusions

In summary, a one-step strategy for preparing DNA-Au hybrids as SERS active substrates by simple mixing of DNA and Au colloids was demonstrated. The Au NPs were self-assembled onto the DNA strands by electrostatic interactions bewteen the negatively charged phosphate DNA backbone and positively charged Au NPs. DNA network provided a better template for the formation of compact and uniform nanostructures by the electrostatic assembly of Au NPs on DNA strands with a well-defined 2-3 nm nanogap in high yields. SERS measurements of small-molecule probes, such as R6G, 4-ATP, Py and TNT were performed on these DNA-Au hybrid substrates with significant enhanced sensitivity and reproducibility compaered to the Au NPs solely. Great Raman enhancements achieved on these new substrates are believed to be the result of the formation of nanogap structures.

Acknowledgements

This work is supported by the National Science Foundation of China (No. 20871089, 21271136), the Important Project of Anhui Provincial Education Department (KJ2010ZD09) and the Program of Innovative Research Team of Suzhou University (2013kytd02).

Notes and references

[a] *School of Biological and Chemical Engineering, Anhui Key Laboratory of Spin Electron and Nanomaterials, Suzhou University, Suzhou 234000, PR China,*
E-mail: zhlisuzh@163.com
[b] *School of Life Science, Anhui University, Hefei 230039, PR China*
[c] *Institute of Intelligent Machines, Chinese Academy of Sciences, Hefei 230031, China.*

1 P. K. Sudeep, B. I. Ipe, K. G. Thomas, M. V. George, S. Barazzouk, S. Hotchandani and P. V. Kamat, *Nano Lett*., 2002, **2**, 29.
2 L.Wang, X. Shi, N. N. Kariuki, M. Schadt, G. R. Wang, Q. Rendeng, J. Choi, J. Luo, S. Lu and C. J. Zhong, *J. Am. Chem. Soc*., 2007, **129**, 2161.
3 G. R.Wang, L. Wang, Q. Rendeng, J. Wang, J. Luo and C. J. Zhong, *J. Mater. Chem.*, 2007, **17**, 457.
4 R. Kaminker, M. Lahav, L. Motiei, M. Vartanian, R. Popovitz-Biro, M. A. Iron and M. E. van der Boom, *Angew. Chem., Int. Ed.,* 2010, **49**, 1218.
5. Y. C. Cao, R. Jin and C. A. Mirkin, Science, 2002, **297**, 1536.
6 Y. Lu, G. L. Liu and L. P. Lee, *Nano Lett*., 2005, **5**, 5.
7 Y. Fang, N. H. Seong and D. D. Dlott, *Science*, 2008, **321** 388.
8 X. B. Xu, K. Kim, H. F. Li, and D.L. Fan, Adv. Mater. 2012, **24**, 5457.
9 D. K. Lim, K. S. Jeon, J. H. Hwang, H. Kim, S. Kwon, Y. D. Suh and J. M. Nam, Nat Nanotechnol 2011, **6**, 452.
10 M. Pilo-Pais, A. Watson, S. Demers, T. H. LaBean, and G. Finkelstein, Nano Lett. 2014, **14**, 2099.
11 Q. M. Yu, P. Guan, D. Qin, G. Golden and P. M. Wallace, *Nano Lett.,* 2008, **8**, 1923.
12 Y. Q. Wen, C. K. McLaughlin, P. K. Lo, H. Yang, and H. F. Sleiman, *Bioconjugate Chem.* 2010, **21**, 1413.
13 L. L. Sun, D. X. Zhao, Z. Z. Zhang, B. H. Li and D. Z. Shen, *J. Mater. Chem.*, 2011, **21**, 9674.
14 A. G. Wu, Z. Li, H. L. Zhou, J. P. Zheng and E. K. Wang, *Analyst*, 2002, **127**, 585.
15 G. Wei, H. L. Zhou, Z. G. Liu, Y. H. Song, L. L. Sun, T. Yang and Z. Li, *J. Phys. Chem. B*, 2005, **109**, 23941.
16 L. B. Yang, G. Y. Chen, J. Wang, T. T. Wang, M. Q. Li and J. H. Liu, *J. Mater. Chem.*, 2009, **19**, 6849.
17 H. L. Liu, L. B. Yang, H. W. Ma, Z. M. Qi and J. H. Liu, *Chem. Commun.*, 2011, **47**, 9360.
18. W. Kubo, and S. Fujikawa, *Nano Lett.*, 2011, **11**, 8.
19. T. Jesse, P. Pavaskar, P. M. Echternach, R. E. Muller and S. B. Cronin, *Nano Lett.*, 2010, **10**, 2749.
20. L. D. Qin, S. L. Zou, C. Xue, A. Atkinson, G. C. Schatz, and C. A. Mirkin, *Proc. Natl Acad. Sci*. 2006, **103**, 13300.
21. X. M. Qian, X. H. Peng, D. O. Ansari, Q. Yin-Goen, G. Z. Chen, D. M. Shin, L. Yang, A. N. Young, M. D. Wang and S. M. Nie, *Nature Biotechnol*. 2008, **26**, 83.

22. C. L. Zavaletaa, B. R. Smitha, I. Waltonb, W. Doeringb, G. Davisb, B. Shojaeib, M. J. Natanb, and S. S. Gambhir. *Proc. Natl Acad. Sci.*, 2009, **106**, 13511.
23 D. I. Gittins and F. Caruso, *Angew. Chem. Int. Ed.*, 2001, **40**, 3001.
24 Y. J. Sun, G. Wei, Y. H. Song, L. Wang, L. L. Sun, C. L. Guo, T. Yang and Z. Li, *Nanotechnology,* 2008, **19**, 115604.
25 B. F. Pan, D. X. Cui, C. Ozkan, P. Xu, T. Huang, Q. Li, H. Chen, F. T. Liu, F. Gao, and R. He, *J. Phys. Chem. C*, 2007, **111**, 12572.
26 P. Galletto, P. F. Brevet and H. H. Girault, *J. Phys. Chem. B*, 1999, **103**, 8706.
27 S. Basu, S. K. Ghosh, S. Kundu, S. Panigrahi, S. Praharaj, S. Pande, S. Jana and T. Pal, *J. Colloid. Interf. Sci.*, 2007, **313**, 724.
28 H. Nakao, H. Hayashi, T. Yoshino, S. Sugiyama, K. Otobe and T. Ohtani, *Nano Lett.*, 2002, **2**, 475.
29 J. N. Anker, W. P. Hall, O. Lyandres, N. C. Shah, J. Zhao and R. P. Van Duyne, *Nat. Mater.*, 2008, **7**, 442.
30 F. M. Liu, P. A. Kollensperger, M. Green, A. E. G. Cass and L. F. Cohen, *Chem. Phy. Lett.*, 2006 **430**, 173.
31 X. H. Li, G. Y. Chen, L. B. Yang, Z. Jin and J. H. Liu, *Adv. Funct. Mater*., 2010, 20, 2815.
32 L. B. Yang, H. L. Liu, Y. M. Ma and J. H. Liu, *Analyst*, 2012, 137, 1547.
33 L. S. Jiao, Z. J. Wang, L. Niu, J. Shen, T. Y. You, S. J. Dong and A. Ivaska, *J Solid State Electrochem.*, 2006, **10**, 886.
34 G. F. S. Andrade, M. L. A. Temperini, *J. Raman Spectrosc.*, 2009, **40**, 1989.
35 M. W. Shao, L. Lu, H. Wang, S. Wang, M. L. Zhang, D. Ma, S. T. Lee, *Chem. Commun.*, 2008, 2310.
36 Y. H. Sun, K. Liu, J. Miao, Z. Y. Wang, B. Z. Tian, L. N. Zhang, Q. Q. Li, S. S. Fan, K. L. Jiang *Nano Lett.*, 2010, **10**, 1747.
37 L. B. Yang, L. Ma, G. Y. Chen, J. H. Liu and Z. Q. Tian, *Chem. Eur. J.,* 2010, **16**, 12683.

A table of contents entry

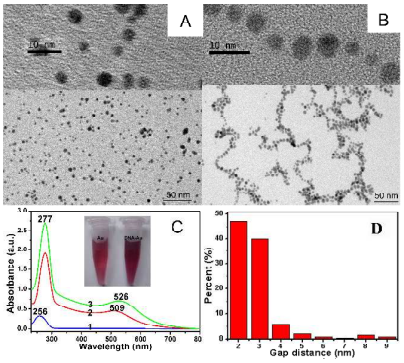

This study provides a one-step strategy for preparing DNA-Au hybrids as SERS active substrates by simple mixing of DNA and Au colloids.